J Solid State Electrochem (2009) 13:565–571
DOI 10.1007/s10008-008-0700-6

ORIGINAL PAPER

The current transient for nucleation and diffusion-controlled growth of spherical caps

Daniel Branco P. · Jorge Mostany · Carlos Borrás · Benjamin R. Scharifker

Received: 6 August 2008 / Revised: 28 September 2008 / Accepted: 29 September 2008 / Published online: 17 October 2008

Abstract The contact angle between growing clusters and the electrode surface is taken into consideration in the description of potentiostatic current transients during nucleation and diffusion-controlled growth of three-dimensional phases. It is shown that the non-dimensional plots of the currents normalized with respect to their maxima, and the nucleation rates obtained from analysis of experimental transients are unaffected by the contact angle. The results obtained reveal, however, that consideration of contact angles different from 90° in analysis of experimental current transients lead invariably to lower number densities of active sites for nucleation.

Keywords Contact angle · Nucleation and growth · Chronoamperometry · Kinetics

Introduction

Phase formation and growth frequently involves the onset of aggregates of atoms or molecules as stable structures that become the centres for the propagation of the new phase, a process supported by material originating from the bulk mother phase. In the formal description of nucleation, the interfacial properties of those small aggregates play a dominant role in determining the excess energy balance, as according to Kelvin equation small clusters would be unstable unless a large deviation from the conditions determining equilibrium between the bulk phases is imposed. The combined contributions due to formation of the new phase and expansion of its surface produces a Gibbs energy maximum defining the radius r^* of the critical nucleus staying in metastable equilibrium with the supersaturated parent phase. The potentiostatic technique allows controlling the system supersaturation by changes in the electrochemical potential, therefore, providing an excellent tool to analyse the conditions that determine the occurrence of electrochemical nucleation processes [1].

The sphere has the minimal surface-to-volume ratio among geometrical shapes, hence, minimizing the interfacial energy for a given extent of new phase formed. Spherical shapes are, thus, frequently considered adequate in nucleation kinetics and growth models. The contact angle θ of the nucleus with the electrode surface is shown in Fig. 1, and its value arises out of thermodynamic and mechanical equilibrium between the Gibbs energies of formation or surface tensions σ involving the interfaces between the electrodeposited metallic phase (m), the electrode surface (e) and solution (s). This equilibrium is expressed by the Young equation [1, 2],

$$\sigma_{m,e} + \sigma_{s,m}\cos\theta - \sigma_{s,e} = 0 \quad (1)$$

Resulting from the mechanical equilibrium of the interfaces involved, we will consider that the contact angle is independent of the size of the growing centre and remains constant throughout the electrocrystallisation process, thus, neglecting effects due to gravitational forces affecting large crystals or line tensions at the three-phase boundary affecting very small clusters [3].

Theoretical treatments of current transients have often assumed that growing nuclei are of hemispherical shape, but in actual terms, this arises only at equal Gibbs energies

Dedicated to Keith Oldham in his 80th birthday

D. Branco P. · J. Mostany · C. Borrás · B. R. Scharifker (✉)
Departamento de Química, Universidad Simón Bolívar,
Caracas, Venezuela
e-mail: benjamin@usb.ve
URL: http://prof.usb.ve/benjamin

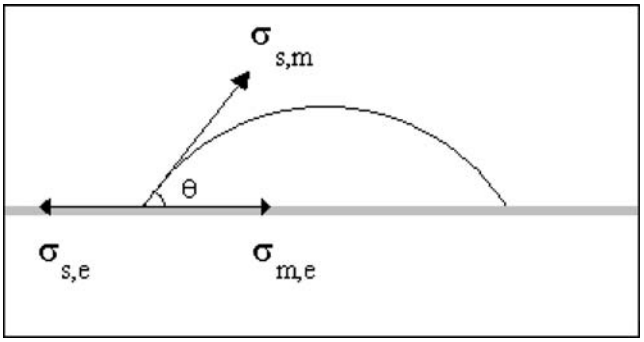

Fig. 1 Contact angle θ between the spherical cap and the electrode surface; the *arrows* depict the tensions σ at the interfaces between electrodeposited metallic phase (*m*), electrode surface (*e*), and solution (*s*)

of formation of the electrode–solution and electrode–deposit interfaces [4]. As this is not necessarily the case, it follows that consideration of contact angles different from 90° is in general needed.

Potential steps to values negative with respect to the $M_s^{z+} + ne_e^- = M_m$ Nernst equilibrium potential lead to the potentiostatic formation and growth of a new metallic phase m on an electrode surface contacting a solution containing metal ions M_s^{z+}. A rising current arises as nuclei of the new three-dimensional phase form and grow by reduction of the metal ions diffusing in solution and reaching its surface. A spherical diffusion profile develops around each growing centre, but as the concentration of metal ions deplete close to the electrode surface, the current reaches a maximum and then decreases approaching that described by the Cottrell equation for semi-infinite diffusion to an unbounded planar electrode. Several models have been proposed to describe the current transient considering either the instantaneous birth of all nuclei at the onset of the potential step, or their progressive appearance with rate A onto a number density N_0 of active sites for nucleation on the electrode surface [4–11]. As stated above, it has been commonly assumed that centres grow with hemispherical shapes.

In this paper, we revisit the standard model of the potentiostatic current transient for three-dimensional nucleation and diffusion controlled growth processes [11] and take into account the effects of the contact angle θ of nuclei with the electrode surface on the kinetic parameters N_0 and A found from analysis of experimental chronoamperometric data. The starting point for such treatment is the expression for the steady-state current of a spherical cap-shaped microelectrode obtained by Alfred and Oldham [12]. The results presented here pave the way for the experimental determination of contact angles θ as well as nucleation rates and active site densities from potentiostatic single steps, using chronoamperometry combined with in situ optical data, but this is beyond the scope of the present work and will be reported elsewhere (Saavedra et al. unpublished).

Diffusion current to a growing spherical cap

Due to their small size during the early stages of electrocrystallisation, growing clusters behave as microelectrodes with steady state mass transfer flux rapidly achieved [13, 14], a condition frequently assumed in describing their potentiostatic growth under diffusion-controlled growth conditions [4–11]. The geometry and mass transfer flux to spherical caps is schematically depicted in Fig. 2. We may discern from the diagram the mass transfer flux in the radial direction normal to the surface of the spherical cap, shown with solid arrows, as well as non-radial fluxes running in directions along the electrode surface, indicated with dashed arrows.

Mass transport by diffusion to spherical cap-shaped microelectrodes onto conducting circular disks surrounded by an infinite planar insulator has been considered by

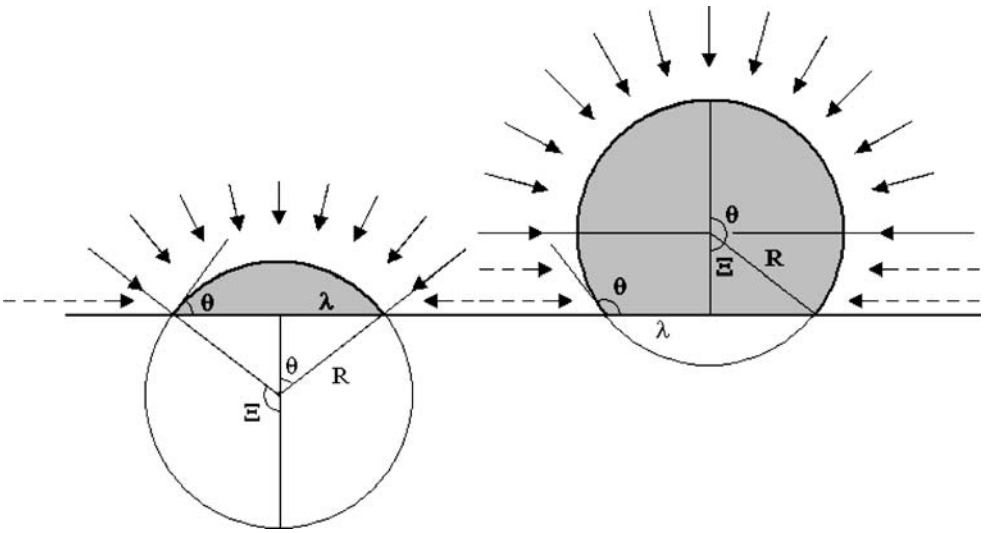

Fig. 2 Lateral view of spherical caps with contact angle smaller (*left*) and larger (*right*) than 90°; the *horizontal solid line* is the electrode surface. Mass transport fluxes are also shown with *arrows*, see text

Alfred and Oldham [12], who obtained an expression of the steady-state current i is a function of the radius of the circular disk λ and the angle Ξ, Fig. 2:

$$i = 4nFDc\lambda \int_0^\infty \left(1 - \tanh(u)\tanh\left(\frac{\Xi u}{\pi}\right)\right) du \tag{2}$$

where nF is the molar charge of the electrodeposited metal, D the diffusion coefficient of the metal ion in solution and c its bulk concentration. Since $\lambda = R\sin(\theta)$ and $\theta = 180° - \Xi$, then Eq. 2 can be written as a function of the radius R of the spherical cap and the contact angle θ,

$$i = 4F(\theta)\sin(\theta)n\mathrm{F}DcR \tag{3}$$

where

$$F(\theta) = \int_0^\infty \left(1 - \tanh(u)\tanh\left(\frac{(\pi - \theta)u}{\pi}\right)\right) du \tag{4}$$

is a numerical factor depending only of the contact angle θ, as shown in Fig. 3. For $\theta = 90°$, all flux is radial and normal to the curved surface, and in this particular case, $F(\theta) = \pi/2$ and Eq. 3 reduces to the well-known steady-state semi-infinite spherical diffusion current to the hemisphere [6, 15, 16]:

$$i = 2\pi n\mathrm{F}DcR \tag{5}$$

The rate of incorporation of metal ions to the spherical cap-shaped growing centre is set by the current; hence, its radius as a function of time is given from the Faraday equation and the molar volume M/ρ of the deposit, relating the current to the volume change $\mathrm{d}V/\mathrm{d}t$,

$$\frac{dV}{dR}\frac{dR}{dt} = \frac{i}{n\mathrm{F}}\left(\frac{M}{\rho}\right) \tag{6}$$

$\mathrm{d}V/\mathrm{d}R$ depends on the geometry of the spherical cap; thus substituting in Eq. 6 the derivative of the spherical cap

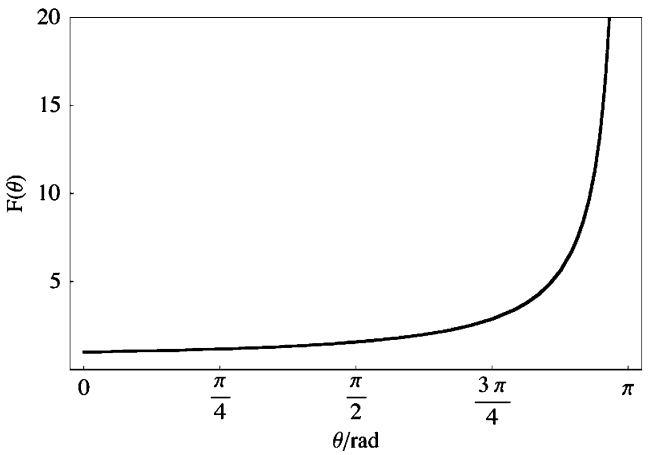

Fig. 3 $F(\theta)$ as a function of the contact angle

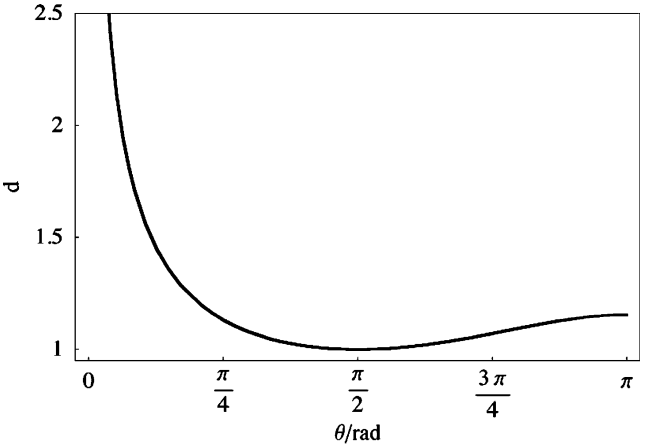

Fig. 4 Behaviour of d with the contact angle

volume $V = (\pi/3)(1 - \cos\theta)^2(2 + \cos\theta)R^3$ and the diffusion current i to the spherical cap (Eq. 3),

$$\pi(1 - \cos\theta)^2(2 + \cos\theta)R^2\frac{dR}{dt} = 4F(\theta)\sin(\theta)DcR\left(\frac{M}{\rho}\right) \tag{7}$$

followed by integration, yields the time-dependent radius R of spherical cap-shaped growing nucleus:

$$R = \left(\frac{F(\theta)\sin\theta}{(1 - \cos\theta)^2(2 + \cos\theta)}\frac{8DcM}{\pi\rho}t\right)^{1/2} \tag{8}$$

which once again, for contact angle $\theta = 90°$, $F(\theta) = \pi/2$, reduces to the known expression for the radius of a growing hemisphere [5, 6], $R = (2DcMt/\rho)^{1/2}$.

Substitution of Eq. 8 into Eq. 3 yields the current i to a single spherical cap-shaped nucleus as a function of time:

$$i = 4n\mathrm{F}Dc\left(\frac{(F(\theta)\sin\theta)^3}{(1 - \cos\theta)^2(2 + \cos\theta)}\frac{8DcM}{\pi\rho}\right)^{1/2} t^{1/2} \tag{9}$$

We may now relate the spherical cap current to that corresponding to the hemisphere writing Eq. 9 as:

$$i = \left(\frac{\pi n\mathrm{F}(2Dc)^{3/2}M^{1/2}}{\rho^{1/2}}t^{1/2}\right)d \tag{10}$$

where

$$d = \left(\frac{16(F(\theta))^3\sin\theta(1 + \cos\theta)}{\pi^3(1 - \cos\theta)(2 + \cos\theta)}\right)^{1/2} \tag{11}$$

is a non-dimensional quantity depending only on the contact angle θ. As shown in Fig. 4 for a given time after birth, the growth currents of spherical cap-shaped nuclei decrease as the contact angle increases from 0° to 90°, then increasing slightly for contact angles rising from 90° to

180°. The minimum current obtains at θ=90°, this particular case with d=1 corresponding to the current of a growing hemisphere reported in previous studies [4–11].

The current transient

In multiple nucleation it is necessary to consider the interactions between growing nuclei. They develop around them spherical diffusion zones and eventually these overlap into a single planar diffusion zone covering the entire electrode surface [5, 9, 17]. To account for these interactions the concept of planar diffusion zones has been introduced [5, 6, 11], defined as circular areas to which are transported, by planar diffusion, the same amount of electroactive material diffusing to the spherical cap by 3D diffusion. Each nucleus then grows with the electroactive material arriving to its corresponding planar diffusion zone, eventually overlapping with those corresponding to the growth of other nuclei. The current transient is thus given at all times as the mass-transfer current to a planar electrode with area corresponding to that of the diffusion zones, taking into account their overlap.

The area of planar diffusion zones can be calculated from the overall mass balance [1, 9] or locally [6, 11], equating the diffusive flux to a spherical cap Eq. 10 with that to a planar diffusion zone:

$$\left(\frac{\pi n\mathrm{F}(2Dc)^{3/2}M^{1/2}}{\rho^{1/2}}t^{1/2}\right)d=\frac{n\mathrm{F}D^{1/2}c}{\pi^{1/2}t^{1/2}}\left(\pi r_d^2\right) \tag{12}$$

where πr_d^2 is the area of the diffusion zone; its radius r_d is:

$$r_d=(dkDt)^{1/2} \tag{13}$$

where $k=(8\pi cM/\rho)^{1/2}$. For an electrode surface with uniformly distributed nucleation sites, the overlap of planar diffusion zones can be taken into account with the Avrami–Evans–Kolmogorov theorem, see, e.g. [5, 6, 10, 11], and the fraction S of surface covered by diffusion zones is given by:

$$S=1-\exp(-bd\Theta(At)t) \tag{14}$$

where $b=N_0\pi kD$ and $\Theta(At)=1-\left(1-\mathrm{e}^{-\mathrm{At}}\right)/\mathrm{At}$. The current density I is then expressed in terms of the number density of active sites, the nucleation rate and the contact angle as the current to a plane electrode of area S:

$$I=\frac{a}{t^{1/2}}\left[1-\exp(-bd\Theta(At)t)\right] \tag{15}$$

where $a=n\mathrm{F}D^{1/2}c/\pi^{1/2}$. Theoretical current transients for various values of the contact angle θ according to Eq. 15 are shown in Fig. 5. In agreement with the result formulated above for the current to a single growing spherical cap, the current falls as contact angles raise from 0° to 90° and increases for contact angles from 90° to 180°. d=1 for θ=90°, and Eq. 15 reduces to the equation proposed by Scharifker and Mostany [11] for hemispheres.

For hemispherical shaped growing nuclei, for which d=1 in Eq. 15, the number density of active sites N_0 and the nucleation rate A may be obtained from analysis of the current maximum I_m and the time corresponding to the maximum t_m in single potential step experiments [11]. For hemispherical growing centres, Hyde and co-workers [18] have reported that a regression analysis of the whole current transient yields a family of pairs of values A and N_0 that fit the curve satisfactorily. However, in the general case, with contact angles θ other than 90° and $d\neq1$, since b and d appear as a product in the exponential term in Eq. 15, then it is not possible to resolve them from regression analysis of current transients alone. We develop below the analysis of the current maximum, leading to the numerical resolution of an equation containing the nucleation rate A on the one hand, resolved from N_0 and θ on the other. Referring to Eq. 15, however, we anticipate two major conclusions arising from the consideration of the contact angle θ together with N_0 and A in current transient analysis, namely that the measured values of A obtained will remain unaffected by θ, indicating invariance of the measurement of nucleation rates with the subsequent growth shapes and that the values of N_0 obtained from current transient analysis will be lower at $\theta\neq\pi/2$, as the values of d will invariably be above unity, Fig. 4. Whereas experimental methods have been proposed for measuring contact angles of single nuclei [19], independent determination of N_0 and θ cannot be accomplished from chronoamperometric data alone in multiple nucleation experiments; thus, additional experimental variables are

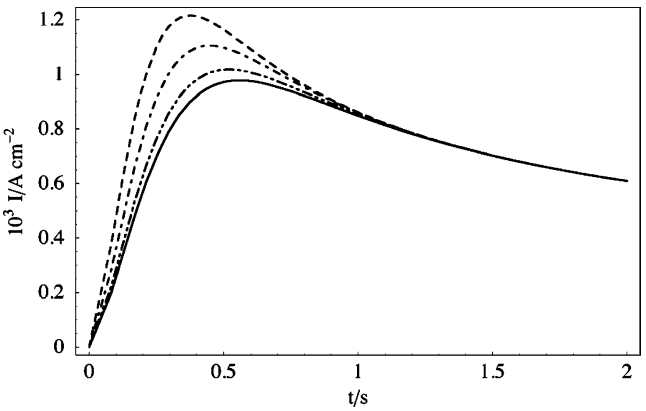

Fig. 5 Theoretical current transients for contact angles θ=11.25° (- -), 22.5° (---), 90° (—) and 157.5° (----), calculated for deposition of silver from 5 mM Ag^+ solution, with $D=1\times10^{-5}$ cm^2 s^{-1}, A=4 s^{-1} and $N_0=5.0\times10^6$ cm^{-2}

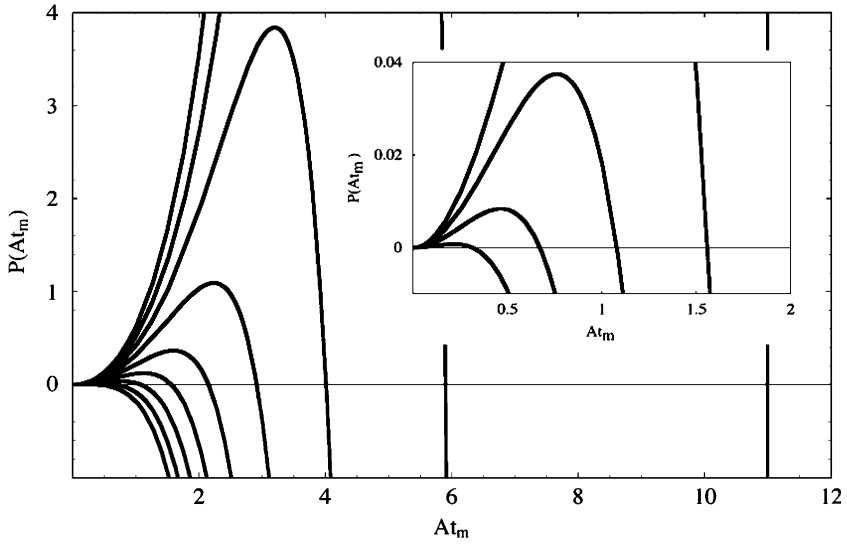

Fig. 6 $P(At_m)$ as a function of At_m for (below the x-axis, from *left* to *right*) κ=1.9, 1.8, 1.7, 1.6, 1.5, 1.4, 1.3, 1.2 and 1.1. The curves for κ=1.2 and 1.1 run over the scale; the insert details the curves for κ=1.9, 1.8, 1.7 and 1.6

required for this, such as optical measurements as it will be reported elsewhere (Saavedra et al. unpublished).

The current maximum

Equating the time derivative of Eq. 15 to zero to find t_m and evaluating at this value leads after rearrangement to the system of non-linear equations (Eqs. 16.1 and 16.2):

$$-bdt_m\Theta(At_m) = \ln\left(1 - \frac{I_m t_m^{1/2}}{a}\right) \tag{16.1}$$

$$\frac{I_m}{2t_m} = \left(\frac{a}{t_m^{1/2}} - I_m\right) bd\left(1 - e^{-At_m}\right) \tag{16.2}$$

Solving Eqs. 16.1 and 16.2 for bd and equating, we obtain:

$$\frac{1 - 1\Big/\left(1 - I_m t_m^{1/2}\Big/a\right)}{2\ln\left(1 - I_m t_m^{1/2}\Big/a\right)} = \kappa = \frac{1 - e^{-At_m}}{\Theta(At_m)} \tag{17}$$

The right hand side in Eq. 17 is expressed in terms of At_m, whereas the left hand side, which we may denote as κ, contains the term $I_m {t_m}^{1/2}/a$, in which all quantities may be experimentally determined. For the limiting cases of instantaneous and progressive nucleation, the values of $I_m {t_m}^{1/2}/a$ are well known [5, 6, 11], 0.7153 and 0.9034, respectively, and consideration of θ does not affect these values, as shown below. The values of κ for instantaneous and progressive nucleation are obtained substituting the respective values in Eq. 17, yielding

$$\kappa = 1 \text{ for instantaneous nucleation} \tag{18}$$

and

$$\kappa = 2 \text{ for progressive nucleation} \tag{19}$$

κ is, thus, a convenient semi-quantitative criterion for characterisation of the nucleation process. After rearrangement, Eq. 17 becomes:

$$[At_m(1-\kappa) + \kappa]\exp(At_m) - At_m - \kappa = 0 \tag{20}$$

Equation 20 has a trivial solution at At_m=0 for all values of κ, and a second root at positive values of At_m depending on κ. Solving numerically Eq. 20 to obtain this root and dividing by the time of the maximum current t_m yields the nucleation rate A. We will denote the left-hand side of Eq. 20 as $P(At_m)$,

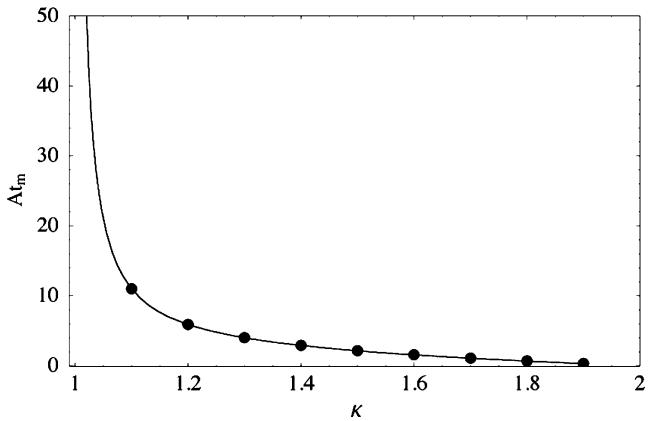

Fig. 7 Roots of Eq. 20, see text, as a function of κ (*continuous line*), and the values of At_m intercepting the x-axis for the corresponding values of κ shown in Fig. 6 (*dots*)

Table 1 Expressions resulting from analysis of the current maximum for instantaneous and progressive nucleation

Instantaneous nucleation	Progressive nucleation
$I = \left(a/t^{1/2}\right)[1 - \exp(-bdt)]$	$I = \left(a/t^{1/2}\right)[1 - \exp(-bdAt^2/2)]$
t_m=1.2564/bd	t_m=(4.6733/Abd)$^{1/2}$
I_m=0.6382a(bd)$^{1/2}$	I_m=0.6144a(Abd)$^{1/4}$
$I_m t_m^{1/2}/a$=0.7133	$I_m t_m^{1/2}/a$=0.9033
κ=1	κ=2
$\left(\frac{I}{I_m}\right)^2 = \frac{1.9542}{(t/t_m)}\left\{1 - \exp\left[-1.2564\left(\frac{t}{t_m}\right)\right]\right\}^2$	$\left(\frac{I}{I_m}\right)^2 = \frac{1.2254}{(t/t_m)}\left\{1 - \exp\left[-2.3367\left(\frac{t}{t_m}\right)^2\right]\right\}^2$

$$P(At_m) = [At_m(1-\kappa)+\kappa]\exp(At_m) - At_m - \kappa \qquad (21)$$

in order to show in Fig. 6 the behavior of the $P(At_m)$ as a function of At_m for several values of κ, between κ=1 for instantaneous nucleation and κ=2 for progressive nucleation. The intercepts of $P(At_m)$ with the x-axis in Fig. 6 correspond to the respective values of At_m satisfying Eq. 20. These roots, calculated using the Newton–Raphson method, are plotted in Fig. 7 versus their corresponding values of κ. Equation 20 has no root other than the trivial at the instantaneous nucleation limit, but as κ varies from 1 to 2, the resulting At_m values decrease, becoming zero at the limit of progressive nucleation.

The product bd may be evaluated from Eqs. 16.1 and 16.2, with d depending solely on θ as defined in Eq. 11. Since $N_0 = b/\pi kD$, then it follows that hemispherical growth, for which d is minimal, will lead to higher values of N_0 than any other contact angle. It also follows from the discussion above that analysis of the maximum of the current transient does not resolve the individual values of b and d. Moreover, as seen in Fig. 4, evaluation of d does not lead in general to the unequivocal determination of θ, because a given value of d is consistent with two contact angles above approximately 42°, one below and the other above 90°. Resolving b and d and finding univocally θ, however, requires a third independent relationship deriving from experimental measurements relating the area or shape of nuclei with some measurable quantity. Although this is beyond the scope of the present work, the possibility of determining the current of parallel reactions occurring only on the surface of nuclei [20] or the use of time-resolved optical techniques to relate transmittance data with chronoamperometric information as it will be reported elsewhere (Saavedra et al. unpublished) could provide feasible methods to obtain separately the kinetic parameters A, N_0 as well as θ.

Instantaneous and progressive nucleation

Instantaneous and progressive nucleation are limiting cases of Eq. 15 [11], with slow nucleation on a large number of active sites ($A \to 0$ and $N_0 \to \infty$) leading to progressive nucleation and fast nucleation on a small number of active sites ($A \to \infty$ and $N_0 \to 0$) to instantaneous nucleation. The corresponding current transients, with expressions for the respective values of I_m and t_m, the parameters relating them and reduced-variable plots [5, 6, 11], are given in Table 1. Non-dimensional plots with various values of κ together with the instantaneous (upper solid curve, κ=1) and progressive nucleation (lower solid curve, κ=2) limits are shown in Fig. 8. It is verified that both I_m and t_m depend on θ by way of d; nonetheless, it is noteworthy that the various tools available to characterise the nucleation process in relation to those limiting cases, namely evaluation of $I_m t_m^{1/2}/a$ or κ, and $(I/I_m)^2$ vs. t/t_m plots, are all independent of θ.

Conclusions

The contact angle of growing nuclei with the electrode surface has been considered in the description of potentiostatic current transients arising from nucleation and three-dimensional diffusion-controlled growth processes. While our discussion here has been based upon a particular formulation of the planar diffusion zones model [11] among

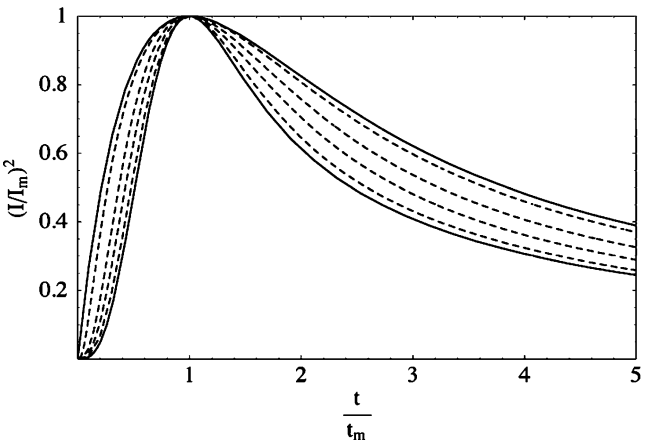

Fig. 8 $(I/I_m)^2$ vs t/t_m non-dimensional plots for (from *top* to *bottom*, *dashed curves*), κ=1.04, 1.18, 1.38 and 1.72. *Solid curves* correspond to the non-dimensional expressions for instantaneous (κ=1, top) and progressive nucleation (κ=2, *bottom*), see Table 1

the several others also available [4–10], the conclusions reached are general and readily extend to other formulations. For given number densities of active sites on the surface and nucleation rates, hemispherical-shaped nuclei will show the smaller values of current. We have shown that while taking into account contact angles differing from 90° in the analysis of current transients will invariably lead to lower number densities N_0 of active sites for nucleation, the nucleation rates A obtained remain unaffected by the contact angle. Furthermore, the non-dimensional expressions for instantaneous and progressive nucleation remain invariant with the contact angle. We have also shown that the contact angle cannot be resolved univocally from the current transient analysis presented, requiring measurement of additional quantities, as described elsewhere (Saavedra et al. unpublished).

Acknowledgements We are grateful to M. Milo and O. Rojas for assistance, and the members of the Electrochemistry laboratory at Simon Bolivar University for fruitful discussions.

References

1. Scharifker BR, Mostany J (2003) In: Bard AJ, Stratmann M, Calvo EJ (eds) Encyclopedia of electrochemistry. vol. 2. Wiley, New York, p 512
2. Milchev A (2002) Electrocrystallization: fundamentals of nucleation and growth. Kluwer, Dordrecht, p 18
3. Mostany J, Mozota J, Scharifker BR (1984) J Electroanal Chem 177:25. doi:10.1016/0022-0728(84)80208-9
4. Abyaneh MY (1991) Electrochim Acta 36:727. doi:10.1016/0013-4686(91)85163-2
5. Scharifker BR, Hills G (1983) Electrochim Acta 28:879. doi:10.1016/0013-4686(83)85163-9
6. Gunawardena G, Hills G, Montenegro I, Scharifker BR (1982) J Electroanal Chem 138:225. doi:10.1016/0022-0728(82)85080-8
7. Sluyters-Rehbach M, Wijenberg JHOJ, Bosco E, Sluyters JH (1987) J Electroanal Chem 236:1. doi:10.1016/0022-0728(87)88014-2
8. Heerman L, Tarallo A (1999) J Electroanal Chem 470:70. doi:10.1016/S0022-0728(99)00221-1
9. Heerman L, Matthijs E, Langerock S (2001) Electrochim Acta 47:905. doi:10.1016/S0013-4686(01)00792-7
10. Matthijs E, Langerock S, Michailova E, Heerman L (2004) J Electroanal Chem 570:123. doi:10.1016/j.jelechem.2004.03.024
11. Scharifker BR, Mostany J (1984) J Electroanal Chem 177:13. doi:10.1016/0022-0728(84)80207-7
12. Alfred LCR, Oldham KB (1996) J Phys Chem 100:2170. doi:10.1021/jp9514685
13. Scharifker BR (1992) In: Bockris JO'M, Conway BE, White RE (eds) Modern aspects of electrochemistry No 22. Plenum, New York, p 467
14. Scharifker BR, Hills GJ (1981) J Electroanal Chem 130:81
15. Gunawardena GA, Hills GJ, Montenegro I (1978) Electrochim Acta 23:693. doi:10.1016/0013-4686(78)80026-7
16. Bard AJ, Faulkner LR (1980) Electrochemical methods. Wiley, New York
17. Hyde ME, Compton RG (2003) J Electroanal Chem 594:1. doi:10.1016/S0022-0728(03)00250-X
18. Hyde ME, Jacobs R, Compton RG (2002) J Phys Chem B 106:11075. doi:10.1021/jp0213607
19. Milchev A, Michailova E, Lacmann R, Müller-Zülow B (1993) Electrochim Acta 38:535. doi:10.1016/0013-4686(93)85009-N
20. Palomar-Pardavé M, Scharifker BR, Arce E, Romero-Romo M (2005) Electrochim Acta 50:4736. doi:10.1016/j.electacta.2005.03.004